Measuring Ventricular Width on Cranial Computed Tomography: Feasibility of Dose Reduction in a Custom-Made Adult Phantom

Ventrikelweitenmessung bei Computertomografien des Schädels: Durchführbarkeit der Dosisreduktion in einem individuell angefertigten Erwachsenenphantom

Authors D. Daubner[1], S. Spieth[2], J. Cerhova[1], J. Linn[1], K. Kirchhof[3]

Affiliations
[1] Department of Neuroradiology, Carl Gustav Carus Medical School, University of Dresden, Germany
[2] Department of Radiology, Carl Gustav Carus Medical School, University of Dresden, Germany
[3] Department of Diagnostic and Interventional Radiology and Neuroradiology, Hospital of Chemnitz, Germany

Key words
- brain
- radiation dose
- CT-spiral
- ventricular width
- hydrocephalus
- adults

received 29.11.2014
accepted 17.7.2015

Bibliography
DOI http://dx.doi.org/10.1055/s-0041-106072
Published online: 13.11.2015
Fortschr Röntgenstr 2016; 188: 73–81 © Georg Thieme Verlag KG Stuttgart · New York · ISSN 1438-9029

Correspondence
Herr Dr. Dirk Daubner
Abteilung Neuroradiologie,
Universitätsklinikum Dresden
Fetscherstraße 74
01307 Dresden
Germany
Tel.: ++ 49/03 51/45 81 84 04
Fax: ++ 49/03 51/4 58 43 70
Dirk.Daubner@uniklinikum-dresden.de

Zusammenfassung

Ziel: Die Abschätzung einer möglichen Dosisreduktion zur zuverlässigen Messung der Ventrikelweite bei computertomografischen Verlaufskontrollen von Erwachsenen mit Hydrozephalus unter Verwendung eines individuell angefertigten Phantoms.

Material und Methoden: Als Messphantom diente eine mit Gelatine gefüllte adulte Schädelkalotte, in der 2 Möhren als Seitenventrikel eingebettet waren. Das Phantom wurde mit 2 CT-Scannern (LightSpeed Ultra, GE und Somatom Sensation, Siemens) jeweils 11-mal untersucht, wobei Röhrenströme von 380/400, 350, 300, 250, 200, 150 und 100 mA sowie -spannungen von 140, 120, 100 und 80 kV verwendet wurden. Zwei Untersucher, die zu den Scanparametern verblindet waren, bestimmten im Konsensusprinzip die Möhrenbreite an vier Stellen. Die bei 380/400 mA und 140 kV durchgeführte Breitenmessung der Möhren diente als Referenz. Messwerte erhielten 1 Punkt, wenn sie nicht mehr als 0,5 mm von der Referenz abwichen. Maximal konnten 4 Punkte erreicht werden.

Ergebnisse: Der Zusammenhang zwischen der Röntgendosis und der korrekten Breitenmessung der Möhren (Seitenventrikel) kann durch eine quadratische Regressionsfunktion beschrieben werden. Mit abnehmender Strahlendosis steigt das Pixelrauschen und die Genauigkeit der Messergebnisse sinkt. Ausgehend von einem Röhrenstrom von 380/400 mA und einer -spannung von 140 kV kann beim LightSpeed Ultra die Dosis um 76 % und beim Somatom Sensation um 80 % reduziert werden, wenn ein Fehler von 37,5 % (Score = 2,5) für die korrekte Breitenmessung der Möhren akzeptiert wird.

Schlussfolgerung: Verglichen mit dem Standardprotokoll (120 kV und 400 mA) führt in diesem Modell eine Reduktion der Strahlendosis um 48 % beim LightSpeed Ultra und um 52 % beim Somatom Sensation, verglichen mit dem Standardprotokoll, zu einer zuverlässigen Messung der Ventrikelweite.

Abstract

Purpose: To estimate feasible dose reduction to reliably measure ventricular width in adults with hydrocephalus in follow-up cranial computed tomography (CCT) using a custom-made phantom.

Materials and Methods: A gelatine-filled adult calvarium with embedded central fibers of two carrots representing the lateral ventricles was used as a phantom. The phantom was scanned 11 times with two CT scanners (LightSpeed Ultra, GE and Somatom Sensation, Siemens), using tube currents of 380/400, 350, 300, 250, 200, 150 and 100 mA, and tube voltages of 140, 120, 100 and 80 kV. The width of the carrots was measured at four sites in consensus decision of two principle investigators blinded to the scan parameters. Values measured at 380/400 mA and 140 kV served as a reference for the width of the ventricles. Measurements received 1 point if they did not differ more than 0.5 mm from the reference values. A maximum score of 4 could be achieved.

Results: The relationship between the correct width measurement of the carrots (lateral ventricles) and the radiation dose can be described by a quadratic regression function. Pixel noise increases and accuracy of measurements decreases with a lower radiation dose. Starting from a tube current of 380/400 mA and a tube voltage of 140 kV, the dose can be reduced by 76 % for LightSpeed Ultra and by 80 % for Somatom Sensation provided that a margin of error of 37.5 % (score = 2.5) for correct width measurement of the carrots is accepted.

Conclusion: Lowering the radiation dose by up to 48 % for LightSpeed Ultra and by 52 % for Somatom Sensation, compared to the standard protocol (120 kV and 400 mA) still allowed reliable measurements of ventricular widths in this model.

Key Points:
- There is a quadratic relationship between correct width measurements of lateral ventricles and radiation dose in CT.

tom Sensation noch zu einer zuverlässigen Messung der Ventrikelbreite.

Kernaussagen:

- Es besteht ein quadratischer Zusammenhang zwischen Röntgendosis und der korrekten Weitenmessung der Seitenventrikel in der CT.
- Eine Dosisreduktion führt zu einem Anstieg des Pixelrauschens sowie des Fehlers für die korrekte Ventrikelweitenmessung.
- Aufgrund des großen Dichteunterschieds zwischen Liquor und Hirnparenchym scheint eine Dosisreduktion zur Ventrikelweitenbestimmung in der CT möglich und sollte durchgeführt werden.

- Reduction of radiation dose results in increased pixel noise and increased error for correct ventricle width measurement.
- Due to a considerable attenuation difference between cerebrospinal fluid and brain parenchyma, a dose reduction for the determination of ventricular size in CT seems feasible and should be performed.

Citation Format:

- Daubner D, Spieth S, Cerhova J et al. Measuring Ventricular Width on Cranial Computed Tomography: Feasibility of Dose Reduction in a Custom-Made Adult Phantom. Fortschr Röntgenstr 2016; 188: 73–81

Introduction

Due to its wide availability, cerebral computed tomography (CCT) is often used in the clinical routine to monitor the width of the ventricles in patients with hydrocephalus [1]. CCT provides additional information regarding the position of ventricular drains and their possible complications. An increased number of follow-up CTs can result in a considerable cumulative radiation dose, and consequently in an increased stochastic risk for genetic defects or development of X-ray induced malignomas in the course of a lifetime [1 – 4].

The ocular lens is a radiosensitive organ due to its limited regenerative capacity. Therefore, particular consideration should be given to CT scans of the head [5]. Despite gantry angulation parallel to the orbitomeatal line and the use of sequential scanning techniques reducing overbeaming and overranging, there remains a scattered radiation exposure of up to 10 % compared to CT scans performed without these techniques. The application of external eye lens protectors or fractional scanning techniques enables a further dose reduction of approximately 50 % [5 – 7]. However, several studies showed that there is no evidence of a minimal threshold dose for radiation-induced cataract [8]. Hence it must be assumed that even low X-ray doses contribute to ocular lens damage.

We hypothesized that it should be possible to decrease radiation dose in follow-up CCTs in adult patients with hydrocephalus due to considerable attenuation differences between cerebral white matter and the sharply defined ventricles. Thus, we aimed to estimate the minimal dose required to reliably measure ventricular width in adults using a custom-made phantom.

Materials and Methods

Reference values

In order to establish the phantom reference values for the mean attenuation of cerebral white matter, cerebrospinal fluid and the width of the lateral ventricles were retrospectively derived from regular non-enhanced CCTs of 30 adults aged between 18 – 85 years randomly chosen from our digital picture archive. The CT scans were performed with the multislice-CT scanners, LightSpeed Ultra (GE Healthcare, Little Chalfont, United Kingdom) and Somatom Sensation (Siemens Healthcare, Forchheim, Germany). A tube voltage of 120 kV and a tube current of 238 ± 47 mA (mean ± standard deviation of the mean) were used for the LightSpeed Ultra scanner and a tube voltage of 140 kV and tube current of 241 ± 47 mA were used for the Somatom Sensation scanner.

The width of the frontal horn and the cella media of the lateral ventricles were determined with our regular picture archiving and communication system (PACS; IMPAX, AGFA HealthCare, Mortsel, Belgium) as delineated in **Fig. 1a, b**. In addition, the attenuation of the cerebrospinal fluid in lateral ventricles and of white matter in the semioval center was determined (**Fig. 1b, c**). All measurements were determined once in consensus decision by two principle investigators.

Custom-made phantom

The study was performed using the following custom-made phantom previously described in the literature [9]: 64 g of gelatine (Platagel, Hela Gewürzwerk, Hermann Laue GmbH & Co. KG, Ahrensburg, Germany) were dissolved in 800 ml of hot water, 2.6 ml of contrast medium (Ultravist 300, Bayer Vital, Leverkusen, Germany) were added and 400 ml of the solution were poured into an adult calvarium. The contrast medium was supplied to the gelatine-water mixture in order to obtain a comparable attenuation to

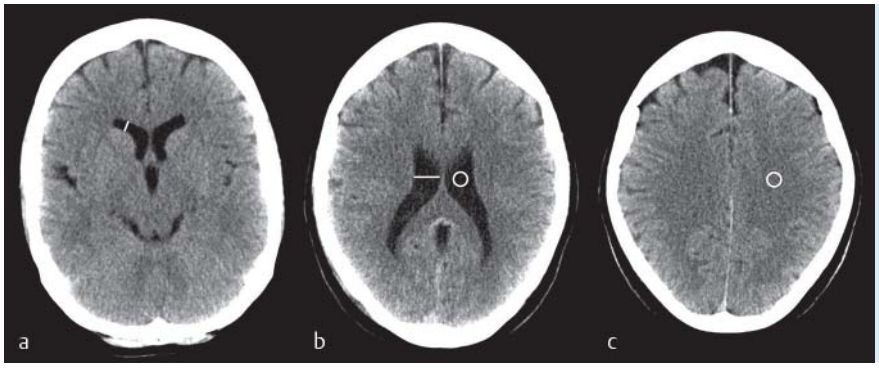

Fig. 1 Exemplary position of width measurement of the lateral ventricles **a**, **b** and the attenuation measurements of the cerebrospinal fluid in the lateral ventricles and of the white matter in the semioval center **b**, **c** in reference patients.

Abb. 1 Exemplarische Position der Weitenmessung der Seitenventrikel **a**, **b** und Dichtemessung des Liquors im Seitenventrikel sowie der weißen Substanz im Centrum semiovale **b**, **c** für die Referenzpatienten.

LightSpeed Ultra			Somatom Sensation		
kV/mA	$CTDI_{Vol}$ (mGy)	mean score	kV/mA	$CTDI_{Vol}$ (mGy)	mean score
140 / 380	109.69	4.00 ± 0.00	140 / 400	83.76	4.00 ± 0.00
140 / 350	101.04	3.77 ± 0.53	140 / 350	73.29	3.64 ± 0.58
140 / 300	86.60	3.50 ± 0.51	140 / 300	62.82	3.27 ± 0.75
120 / 400	84.70	3.09 ± 0.53	120 / 400	55.04	3.09 ± 0.68
120 / 350	74.11	3.18 ± 0.66	140 / 250	52.35	3.46 ± 0.74
140 / 250	72.17	3.27 ± 0.55	120 / 350	48.16	3.46 ± 0.60
120 / 300	63.52	3.14 ± 0.94	140 / 200	41.88	3.32 ± 0.65
140 / 200	57.73	3.18 ± 0.80	120 / 300	41.28	3.36 ± 0.66
100 / 400	54.49	2.55 ± 1.06	120 / 250	34.40	3.27 ± 0.63
120 / 250	52.93	2.95 ± 0.95	100 / 400	32.88	3.14 ± 0.83
100 / 350	47.68	2.59 ± 0.85	140 / 150	31.41	3.09 ± 0.61
100 / 300	40.87	2.91 ± 1.23	100 / 350	28.77	2.50 ± 0.96
140 / 150	40.58	3.14 ± 0.77	120 / 200	27.52	2.91 ± 0.61
120 / 200	39.68	2.82 ± 0.91	100 / 300	24.66	2.41 ± 0.85
100 / 250	34.06	2.59 ± 1.14	140 / 100	20.94	3.14 ± 0.89
80 / 400	30.50	2.41 ± 0.96	120 / 150	20.64	2.82 ± 0.96
120 / 150	29.76	2.86 ± 0.71	100 / 250	20.55	2.55 ± 0.67
140 / 100	27.05	3.05 ± 1.13	100 / 200	16.44	2.50 ± 0.91
80 / 350	26.68	2.09 ± 1.11	80 / 400	16.04	2.59 ± 0.80
100 / 200	25.53	2.64 ± 1.22	80 / 350	14.04	2.46 ± 1.18
80 / 300	21.43	2.50 ± 1.10	120 / 100	13.76	2.18 ± 1.01
120 / 100	19.84	2.55 ± 0.80	100 / 150	12.33	2.18 ± 1.10
100 / 150	19.15	2.50 ± 1.06	80 / 300	12.03	1.77 ± 1.15
80 / 250	17.86	1.86 ± 0.99	80 / 250	10.03	2.14 ± 1.21
80 / 200	14.29	2.09 ± 0.81	100 / 100	8.22	2.05 ± 1.17
100 / 100	12.76	2.36 ± 1.09	80 / 200	8.02	2.27 ± 0.77
80 / 150	10.72	1.82 ± 0.96	80 / 150	6.01	1.86 ± 0.83
80 / 100	7.15	2.18 ± 1.10	80 / 100	4.01	1.86 ± 1.08

Table 1 Overview of the different combinations of tube voltage and tube current used with the LightSpeed Ultra and Somatom Sensation scanner arranged according to descending radiation doses. The corresponding scores of corrected ventricular width measurements are shown.

Tab. 1 Überblick über die beim LightSpeed Ultra und Somatom Sensation verwendeten Kombinationen von Röhrenspannung und -strom geordnet nach absteigender Strahlendosis. Angegeben ist weiter die jeweilige Anzahl richtig gemessener Ventrikelweiten.

that of the white matter of humans. The inner fibers of the carrots were shaped with a knife into pieces with a length of approximately 10 cm and a width of approximately 1 cm. After solidification of the gelatine, the inner fibers of two carrots representing the lateral ventricles were placed onto the gelatine. They were then embedded with the remaining gelatine solution (400 ml).

Phantom measurement

The phantom was examined on two different CT scanners (LightSpeed Ultra and Somatom Sensation). Both CT scanners were calibrated daily prior to the examination of the phantom.

For the LightSpeed Ultra scanner the following scan parameters were used: number of detector rows: 8, collimation: 8 × 1.25 mm, pitch: 1 (table increment: 10 mm per rotation), rotation time: 1 sec, reconstructed slice thickness: 5 mm, number of reconstructed slices: 8, reconstruction kernel: “standard”, field of view: 220 mm, matrix size: 512 × 512 pixel, tube current: 380 mA with a tube voltage of 140 kV, and tube currents of 400 mA, 350 mA, 300 mA, 250 mA, 200 mA, 150 mA und 100 mA with tube voltages of 140 kV, 120 kV, 100 kV and 80 kV. At a tube voltage of 140 kV, only a maximum tube current of 380 mA could be selected on the LightSpeed Ultra scanner. Therefore, 380 mA was the highest tube current used by 140 kV on this scanner.

For the Somatom Sensation scanner the following scan parameters were selected: number of detector rows: 64, collimation: 24 × 1.2 mm, pitch: 1 (table increment: 28.8 mm per rotation), rotation time: 1 sec, reconstructed slice thickness: 4.8 mm, number of reconstructed slices: 6, reconstruction kernel: “H 31s”, field of view: 220 mm, matrix size: 512 × 512 pixel, tube current: 400 mA with a tube voltage of 140 kV, and the tube currents of 400 mA, 350 mA, 300 mA, 250 mA, 200 mA, 150 mA and 100 mA with tube voltages of 140 kV, 120 kV, 100 kV and 80 kV, respectively.

All possible combinations of tube current and tube voltage were tested in each case for both scanners (**Table 1**) and the $CTDI_{Vol}$ values in mGy were specified. 11 scan series on each CT scanner and for each of the 28 different single doses were performed with the phantom.

The helical scan technique was chosen in order to be able to optionally investigate the influence of slice thickness on the measurements. The slice orientation was coronal and axial with respect to the long axis of the carrots.

Data analysis

For each combination of tube current and voltage, the mean attenuation of the gelatine and that of the outer parts of the carrots were measured on 10 consecutive axial slices in a total of 11 regions of interest (ROIs) placed as delineated in **Fig. 2a**. The width of the inner fibers of the carrots was determined on coronal slices at four sites (**Fig. 2b**). All measurements were determined with our regular PACS (IMPAX, AGFA HealthCare, Mortsel, Belgium). Images acquired at the highest radiation dose (tube voltage of 140 kV and tube current of 380 mA / 400 mA) served as a reference. To ensure that corresponding measurements were carried out exactly at the same position in each dataset, the measurement lines of the reference scans were copied and pasted into each of the other datasets. The measurement lines were adjusted to the edges of the carrots in consensus decision of two principle investigators blinded to the scan parameters.

The measured width of the carrots was regarded as within an acceptable range of error, if it did not differ from the reference values by more than ± 0.5 mm. This range was determined after

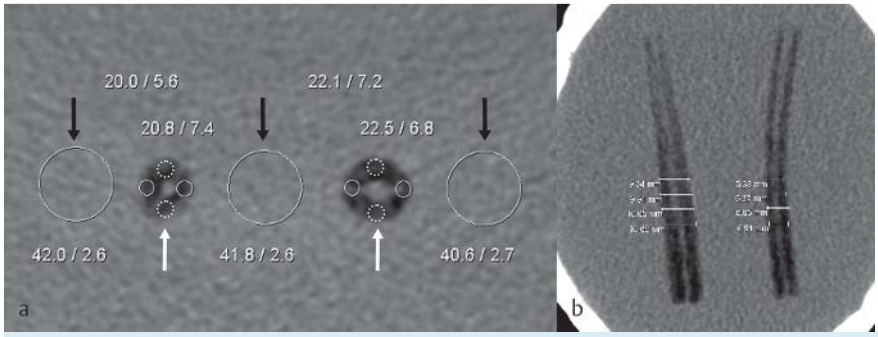

Fig. 2 Size and position of the regions of interest (ROIs) which were used to measure the mean attenuation (in Hounsfield Units) of the carrots (ROIs labeled with white arrows) and gelatin (ROIs labeled with black arrows) on 10 consecutive axial slices acquired with the LightSpeed Ultra scanner **a**. Mean attenuation values of ROIs placed at 12 and 6 o'clock (dashed circles) in the carrots are not shown for the sake of clarity. Width measurements of the carrots at 4 sites on each side acquired with the LightSpeed Ultra scanner **b**.

Abb. 2 Größe und Position der Messfelder (Regions of Interest, ROIs), mit denen die mittlere Röntgendichte (in Hounsfield-Einheiten) von Möhren (mit weißen Pfeilen markiert) und Gelatine (mit schwarzen Pfeilen markiert) auf 10 konsekutiven axialen Schnittbildern mit dem LightSpeed-Ultra-Scanner bestimmt wurde **a**. Die mittleren Dichtewerte der bei 6 und 12 Uhr in den Möhren platzierten Messfelder (gestrichelte Kreise) sind zur besseren Übersichtlichkeit nicht abgebildet. Breitenmessung der Möhren mit dem LightSpeed-Ultra-Scanner an 4 Stellen auf jeder Seite **b**.

consultation with our neurosurgeons who consider a change in ventricular size by 1 mm as relevant for their therapeutic decisions. Measurements within this range were judged as a "correct measurement" and resulted in a score of one point each. For each carrot, a maximum score of 4 could be obtained, if measurements at all four sites within one carrot were within the accepted range. If none of the four width measurements was correct compared to the reference, a score of 0 was assessed. The mean score ± standard deviation was determined for each combination of tube current und tube voltage for both scanners.

In each case, the attenuation of the gelatine and the carrots as mean ± standard deviation in Hounsfield Units (HU) as well as the mean scores for the width measurement of carrots ± standard deviation were determined.

The relationship between the number of correct width measurements of the carrots and radiation dose ($CTDI_{Vol}$ values) was statistically analyzed using the Spearman's rank correlation coefficient. Based on visual inspection of the scatter plots, a quadratic curve fit was used to describe the mathematical relationship of these parameters and calculate the goodness of fit (R^2).

Results

Reference measurements in adult patients

Reference measurements in 30 randomly selected CCTs performed in adult patients revealed a mean attenuation of white matter in the semioval center of 27.3 ± 1.2 HU and a mean attenuation of cerebrospinal fluid in the lateral ventricles of 5.9 ± 2.2 HU, resulting in a mean difference of attenuation between cerebral white matter and cerebrospinal fluid of 21.4 HU. The mean widths of the frontal horn and the cella media of the lateral ventricles were 0.8 ± 0.3 cm and 1.2 ± 0.4 cm, respectively.

Phantom measurements

In the phantom, the mean attenuation of the carrots representing the lateral ventricles was 22.1 ± 5.1 HU as measured with the LightSpeed Ultra scanner and 23.9 ± 5.2 HU as measured with the Somatom Sensation scanner. The mean attenuation values for gelatine representing white matter were 41.0 ± 0.7 HU (LightSpeed Ultra) and 45.2 ± 0.9 HU (Somatom Sensation). The differences in the attenuation of gelatine and carrots (white matter and cerebrospinal fluid) were 18.9 HU (LightSpeed Ultra) and 21.3 HU (Somatom Sensation). There were no significant changes in attenuation over time or with different tube voltages and currents. The width measurements of the carrots yielded values between 5.52 and 11.75 mm.

Table 1 shows the $CTDI_{Vol}$ values with different combinations of tube current and tube voltage that were applied with the LightSpeed Ultra and Somatom Sensation scanner. The mean $CTDI_{Vol}$ values of the LightSpeed Ultra scanner were higher by the factor of 1.56 ± 0.14 than the one of the Somatom Sensation scanner. The scanned distance with the LightSpeed Ultra scanner was 1.39 times longer than with the Somatom Sensation scanner due to the different collimation of both scanners. Arranging the different combinations of tube current and tube voltage according to descending radiation doses showed a different sequential arrangement for both scanners (**Table 1**). Doses of 109.69 mGy (with 140 kV / 380 mA, LightSpeed Ultra) and 83.76 mGy (140 kV, 400 mA, Somatom Sensation) served as a reference.

When the tube voltage was reduced at a given tube current, the $CTDI_{Vol}$ values decreased and the pixel noise increased exponentially (**Fig. 3**). By reducing the tube voltage from 120 kV to 80 kV, the mean $CTDI_{Vol}$ values decreased by a factor of 2.83 ± 0.09 (LightSpeed Ultra) and 3.43 ± 0.00 (Somatom Sensation).

A reduction of the tube current at a given tube voltage resulted in a linear decrease of $CTDI_{Vol}$ values (**Fig. 4**) and an exponential increase in pixel noise (**Fig. 3**). With a reduced tube current from 380/400 mA to 100 mA, the $CTDI_{Vol}$ values decreased by a factor of 4.22 ± 0.11 (LightSpeed Ultra) and 4.00 ± 0.00 (Somatom Sensation).

At standard values of 120 kV and 400 mA for a CCT, the applied doses were 84.70 mGy with the LightSpeed Ultra scanner and 55.04 mGy with the Somatom Sensation scanner.

Measurement of carrot (ventricular) width

When reducing the radiation doses ($CTDI_{Vol}$), the score for the correct measurement of carrot (ventricular) width decreased at both scanners by a quadratic correlation (**Fig. 5, 6**).

The correlation analysis between $CTDI_{Vol}$ and score showed a Spearman rank correlation coefficient of 0.88 with a 95 % confidence interval of 0.76 to 0.95 for LightSpeed Ultra (p-value

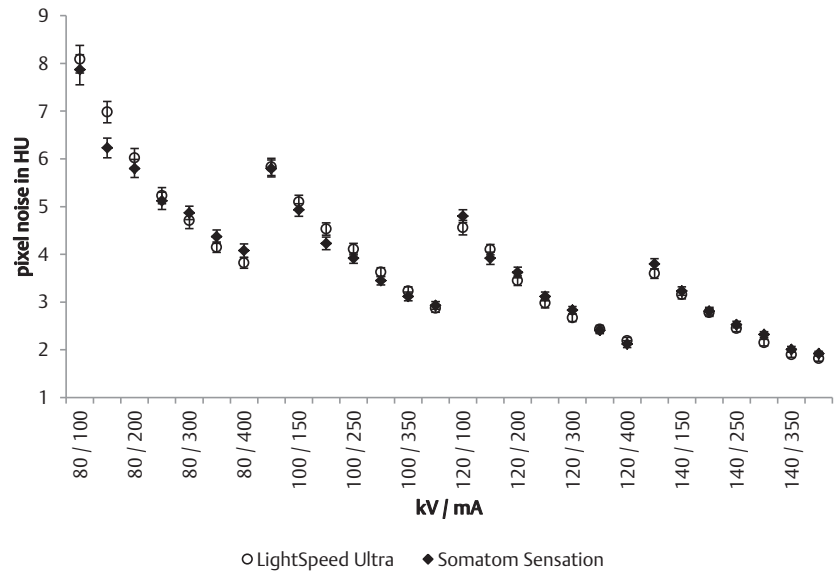

Fig. 3 Pixel noise of gelatine in Hounsfield Units (HU) measured with LightSpeed Ultra and Somatom Sensation in the regions of interest (shown in Fig. 1) at different combinations of tube voltage und tube current (open dots and diamonds with error indicator represent mean values ± standard deviation of the LightSpeed Ultra and the Somatom Sensation scanner, respectively).

Abb. 3 Pixelrauschen der Gelatine in Hounsfield-Einheiten (HE), die in Messfeldern (Regions of Interest) mit dem LightSpeed Ultra und Somatom Sensation bei verschiedenen Kombinationen von Röhrenstrom und -spannung gemessen wurden (offene Punkte und Rauten mit Fehlerindikator geben die Mittelwerte ± Standardabweichung für den LightSpeed-Ultra- und den Somatom-Sensation-Scanner an).

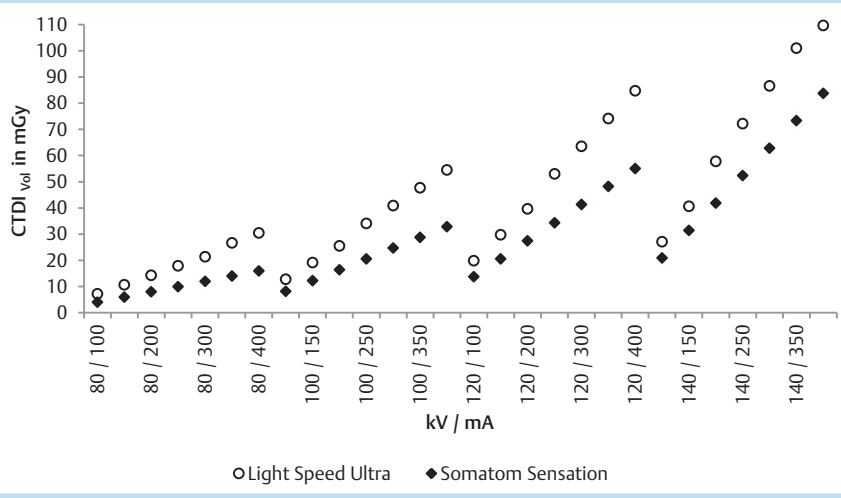

Fig. 4 Radiation doses ($CTDI_{Vol}$ values) measured at different combinations of tube voltage and tube current on the LightSpeed Ultra (open dots) and Somatom Sensation scanner (diamonds).

Abb. 4 Strahlendosen ($CTDI_{Vol}$-Werte), die mit dem LightSpeed Ultra (offene Punkte) und dem Somatom Sensation (Rauten) bei den verschiedenen Kombinationen und Röhrenspannung und -strom gemessen wurden.

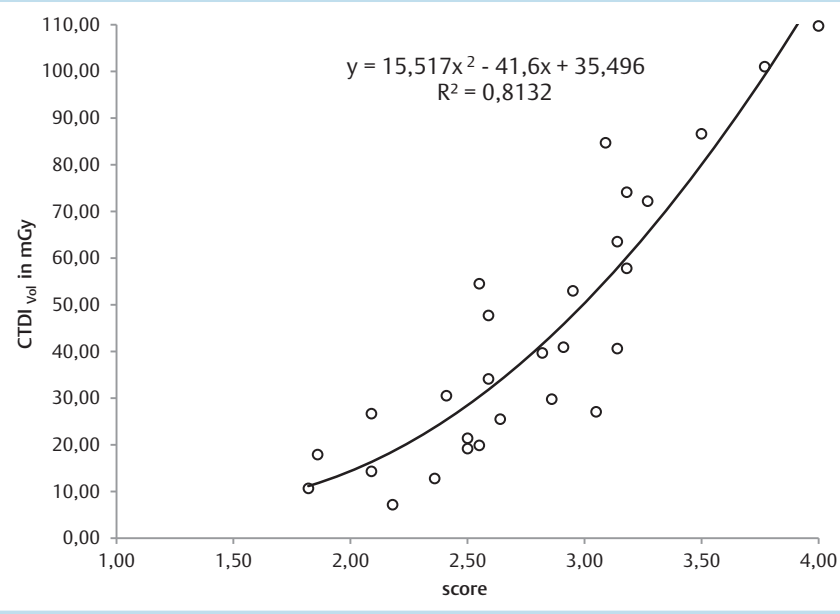

Fig. 5 Correlation between scores of correct ventricular width (X-axis) and radiation doses (Y-axis) measured for the LightSpeed Ultra scanner (labeled with open dots).

Abb. 5 Korrelation zwischen dem Punktwert der korrekten Ventrikelweitenmessung (X-Achse) und der Strahlendosis (Y-Achse) für den LightSpeed-Ultra-Scanner (markiert mit offenen Punkten).

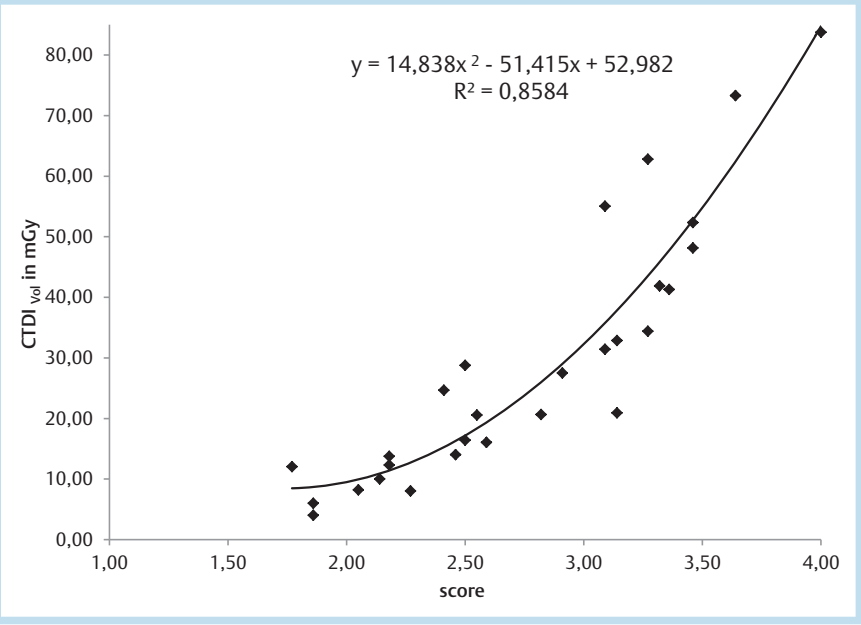

Fig. 6 Correlation between scores of correct ventricular width (X-axis) and radiation doses (Y-axis) measured for the Somatom Sensation scanner (labeled with diamonds).

Abb. 6 Korrelation zwischen dem Punktwert der korrekten Ventrikelweitenmessung (X-Achse) und der Strahlendosis (Y-Achse) für den Somatom-Sensation-Scanner (markiert mit Rauten).

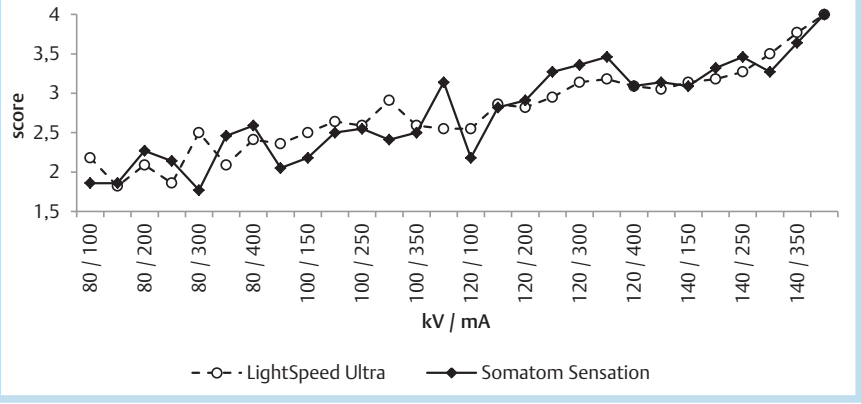

Fig. 7 Scores of correct ventricular width measurements at different combinations of tube voltage and tube current (open dots and diamonds indicate mean scores of the LightSpeed Ultra and the Somatom Sensation scanner, respectively).

Abb. 7 Punktwert korrekter Ventrikelweitenmessungen bei verschiedenen Kombinationen von Röhrenspannung und -strom (offene Punkte und Rauten zeigen die mittleren Punktwerte für den LightSpeed Ultra und den Somatom-Sensation-Scanner).

<0.0001). The Spearman's rank correlation coefficient for Somatom Sensation was 0.93 with a 95 % confidence interval of 0.84 to 0.97 (p-value <0.0001). The goodness of fit of the quadratic regression yielded an R^2 of 0.81 for LightSpeed Ultra and an R^2 of 0.86 for Somatom Sensation.

An increase in tube voltage or tube current leads to an undulant non-linear increase of the score for the correct measurement of carrot (ventricular) width. The score of correct measurements is plotted against the scanning parameters in **Fig. 7**. **Fig. 8, 9** give an impression of the image quality of scans using less than 85 % of the radiation dose compared to scans with a tube voltage of 120 kV and a tube current of 400 mA.

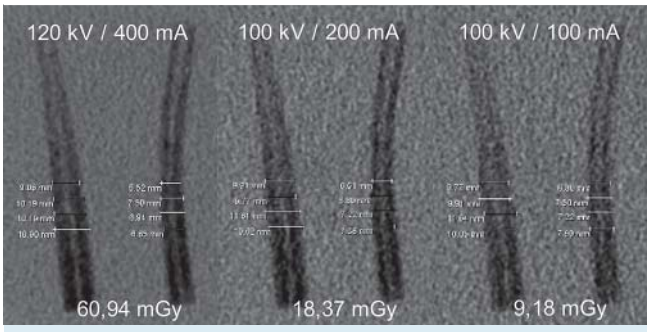

Fig. 8 Image quality of scans acquired on the LightSpeed Ultra scanner using less than 85 % of the radiation dose compared to the reference standard, i. e. a tube voltage of 120 kV and a tube current of 400 mA.

Abb. 8 Bildqualität der Untersuchungen, die der LightSpeed-Ultra-Scanner unter Verwendung von weniger als 85 % der Strahlendosis lieferte, im Vergleich zum Referenzstandard von 120 kV und 400 mA.

Discussion

According to our phantom study, the reduction of radiation exposure is dependent on the lowest score accepted for the correct ventricular width measurement. If, in a setting of 140 kV and 380/400 mA, a score of 3 is adopted as the lowest limit, the dose can be reduced by 57 % for LightSpeed Ultra and by 62 % for Somatom Sensation based on the quadratic regression analysis. If a score of 2.5 is defined as the lowest limit for the correct ventricular width measurement, a dose reduction of 76 % for LightSpeed Ultra and 80 % for Somatom Sensation can be achieved.

In principle, CT radiation dose is directly proportional to the tube current and increases with the square of tube voltage [2, 4, 10]. A

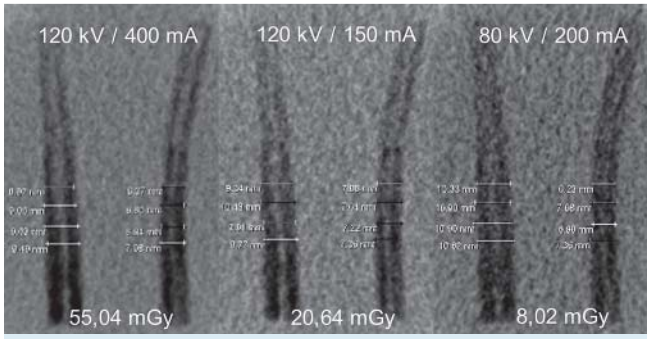

Fig. 9 Image quality of scans acquired on the Somatom Sensation scanner using less than 85 % of the radiation dose compared to the reference standard, i. e. a tube voltage of 120 kV and a tube current of 400 mA.

Abb. 9 Bildqualität der Untersuchungen, die der Somatom-Sensation-Scanner unter Verwendung von weniger als 85 % der Strahlendosis lieferte, im Vergleich zum Referenzstandard von 120 kV und 400 mA.

reduction of these parameters consequently leads to a decrease in the radiation dose, but also to an increase in the image (pixel) noise resulting in deteriorated image quality [11]. While high contrast objects such as bones can be scanned with a significant reduction of radiation dose (more than 50 %) without any relevant loss of information [2, 10, 12], scanning of low contrast objects leads to an impairment of image quality through increasing image noise [1, 4]. Low contrast resolution and detection of details is mainly determined by pixel noise. An increase in pixel noise leads to a decrease in low-contrast detectability. Therefore, low-contrast details on CT images are superimposed by noise [11].

Low-dose protocols of the neurocranium have several limitations, whereby diagnosis of diapedesis of cerebrospinal fluid, subarachnoidal hemorrhage, cerebritis or early stroke may be impaired or completely missed [1]. For the repeated assessment of ventricular width in patients with hydrocephalus, low-dose scanning protocols are often sufficient due to the large attenuation differences of cerebrospinal fluid and cerebral white matter [1].

This study showed that distance measurements to assess carrot width (ventricular width) are more accurate due to the lower image noise at high doses. By reducing the tube voltage, the pixel noise increases, but at the same time it also leads to an increase in image contrast and contrast-to-noise ratio [12, 13]. In daily practice this is mostly used in CT examinations of tissues with a high atomic number (bone or iodine in vessels) due to the photoelectric effect [13, 14]. The attenuation difference between carrots and gelatine in our phantom was relatively low and the average attenuation was in the lower segment of the Hounsfield scale so that the causal photoelectric effect played a minor part. We observed that accurate measurements were obtained at a comparable dose when the phantom was investigated at higher tube voltages and lower tube currents compared with scans at low tube voltages and higher tube currents. High-energy radiation, which is less weakened in the body or in the phantom compared to low-energy radiation, is produced at high tube voltages. This results in more X-ray quanta contributing to image formation, so that image noise is reduced and distance measurements (scores) are more accurate. Cohnen et al. also showed that better image quality is achieved at higher tube voltages [12, 15]. Our data clearly showed an increase in the accuracy of carrot width measurement at higher tube voltages and constant tube current. An increase of the tube current at a low kV value cannot fully compensate for the absorption of the photons.

Starting from our standard values of 120 kV and 400 mA, we found that $CTDI_{Vol}$ values in the phantom can be reduced by 48 % and by 52 % using the LightSpeed Ultra and the Somatom Sensation scanner, respectively, when a margin of error of 37.5 % for the correct width measurement of ventricles is accepted. Other studies showed that for the determination of ventricular size a dose reduction up to 70 % is possible, however with significant image quality reduction in some cases. These analyses were performed in clinical studies and in cadaver or phantom studies and evaluated image quality by changing tube voltage and current [4, 12, 16]. Due to different scanner geometry, filters and interpolation algorithms, sequential combination of tube current, tube voltage and image quality differ between the two scanners when arranged by the resulting radiation dose [14]. For this reason, the scores for the two scanners can vary at the same settings. Thus, the most efficient combination of tube current and tube voltage must be determined individually for each type of scanner [9].

In CT examinations of the neurocranium, sequential and helical techniques are established with advantages and disadvantages. The advantage of the sequential technique is the good gray and white matter differentiation. However, streak artifacts in the posterior fossa increase in the sequential technique and may limit evaluability. In the helical CT technique overranging results in an increased dose, which can be reduced by adaptive collimation by the manufacturer. It was also shown that helical CT results in a lower lens dose and better image quality in the posterior fossa [17, 18]. In our study design the helical scan technique was chosen in order to have the option to investigate the influence of slice thickness on the measurements.

Modulation of the tube current in the direction of the XY- and Z-axis is nowadays standard in modern scanners and adapts the tube current to the dose absorption of the patient (patient's geometry). This normally significantly decreases the radiation exposure of radiosensitive organs while the image quality stays constant [7]. Due to the round sectional profile of the head, dose reduction by tube current modulation in the direction of XY is insignificant in CCT. In the direction of Z, there is little change of X-ray absorption between the skull and the skull base, so that the extent of dose reduction through tube current modulation in the Z-direction is clearly limited [19].

While our phantom study examined the most common variation of radiation dose by adjusting tube current and tube voltage, dose adjustment may also be carried out by varying pitch, scan time, slice thickness and scan volume [2, 4, 10]. Increasing the pitch leads to a reduction of scan time. A helical scanning technique therefore reduces radiation exposure by a factor of 1/pitch. However, increasing the pitch results in an increase in image noise and poorer spatial resolution in the direction of the Z-axis. Our Siemens scanner uses the so-called effective mAs. With an increasing pitch, the effective mAs increases simultaneously and the radiation dose remains the same [7]. In our GE scanner a change in the pitch leads to a change in dose. For this reason, the study was carried out with a pitch of 1 on both scanners to enable comparison. Regarding the complex anatomy of the ventricular system, increasing slice thickness or decreasing scanning volume seems not to be helpful in assessing and monitoring hydrocephalus because of a consecutively reduced spatial resolution.

A further approach to improve image quality in low-dose CT protocols consists of iterative reconstructions, where different calculation procedures reduce image noise [7]. The extent of a possible

further dose reduction with the help of iterative reconstructions in measuring ventricular width should be investigated in further studies.

In CT scans of the neurocranium scan parameters must be adjusted to the individual patient's characteristics, especially the skull size, because they influence the radiation dose and image quality [2, 3, 20]. A thickened calvarium, for example in internal hyperostosis or Paget's disease, can reduce image quality significantly in low-dose protocols [10].

In general, scanning parameters for each cranial CT scan should be adapted to the clinical questions and/or suspected pathological conditions, and the patient's age and size in order to achieve a balance between image quality and the patient's radiation dose [2, 20]. In accordance with the ALARA (as low as reasonably achievable) principle, the lowest possible radiation dose should be applied to answer clinical questions [2, 10]. Of course, imaging modalities without the use of ionizing radiation should be considered in assessing ventricular width in patients with hydrocephalus. In infants ultrasound is the imaging modality of choice to measure ventricular width until the closure of the fontanelles. Beyond this point, magnetic resonance imaging (MRI) should be performed [1, 2].

Study limitations

The major limitation of our study is the use of a phantom, which intrinsically only partially reflects the situation in humans. Although the difference of attenuation between gelatine and carrots correlates well with the one between white matter and cerebrospinal fluid of reference patients, the study phantom could be criticized for the following points:

The mean attenuation of the gelatine was about 2 times higher and the mean attenuation of the carrots was about 4 times higher than that of white matter and cerebrospinal fluid in the reference patients, so that a possible influence of hardening artifacts cannot be completely ruled out but is likely to play a minor role in the low attenuation difference in the reference patient.

In order to produce a realistic attenuation difference between the lateral ventricles and the white matter in the phantoms, contrast agent was added to the gelatine. At decreasing kV values, the iodine contrast increases, so that there is a potential bias of the carrot width measurements. However, since the mean attenuation difference between carrots and gelatine was almost identical at different tube voltages, we can exclude a relevant influence of the small amount of contrast agent on the measurement results.

In addition, contrast agent added to the gelatine was slightly absorbed by the carrots, which led to blurred edges compared to the ones of cerebral white matter and cerebrospinal fluid in the reference patients [9]. The model calvarium did not contain hematopoietic bone marrow and had no surrounding soft tissue, which results in lower X-ray attenuation as in real patients. Thus, our data may overestimate the potential of dose reduction in follow-up CCTs of patients with hydrocephalus [9].

According to our neurosurgeons, even a minimal increase of the size of the lateral ventricles can be an expression of dysfunctional cerebrospinal fluid circulation. Therefore, a deviation of ± 0.5 mm from the reference value was defined as a correct ventricular width measurement. Due to the very small permitted deviation, an influence on the study results due to measurement inaccuracies cannot be excluded.

As another limitation, it has to be taken into account that additional pathological findings, e. g. transependymal cerebrospinal fluid diapedesis, which may occur in patients and cause a certain degree of uncertainty in the measurements, were not present in our phantom.

Conclusion

Our phantom measurements suggest that lowering the radiation dose by up to 48 % for LightSpeed Ultra and 52 % for Somatom Sensation compared to the standard protocol (120 kV and 400 mA) still allows reliable measurements of ventricular widths.

Clinical relevance of the study

- Patients with hydrocephalus frequently undergo multiple cranial follow-up CT-scans.
- Due to a considerable attenuation difference between cerebrospinal fluid and brain parenchyma, low-dose CT protocols are sufficient to assess ventricular size, leading to a reduction in cumulative radiation dose.
- With decreasing radiation dose, the accuracy of ventricular width measurement decreases.

References

1 *George KJ, Roy D.* A low radiation computed tomography protocol for monitoring shunted hydrocephalus. Surg Neurol Int 2012; 3: 103
2 *Karabulut N, Ariyürek M.* Low dose CT: practices and strategies of radiologists in university hospitals. Diagn Interv Radiol 2006; 12: 3 – 8
3 *Huda W, Vance A.* Patient radiation doses from adult and pediatric CT. Am J Roentgenol 2007; 188: 540 – 546
4 *Udayasankar UK, Braithwaite K, Arvaniti M et al.* Low-dose nonenhanced head CT protocol for follow-up evaluation of children with ventriculoperitoneal shunt: reduction of radiation and effect on image quality. AJNR 2008; 29: 802 – 806
5 Radiation Protection of Patients in Cranial Computed Tomography (Gantry Tilt). Recommendation by the German Commission on Radiological Protection, adopted at the 248th meeting of the German Commission on Radiological Protection on 14./15.04.2011, BAnz no. 168 – 09.11.2011
6 *Keil B, Wulff J, Schmitt R et al.* Protection of eye lens in computed tomography – dose evaluation on an anthropomorphic phantom using thermo-luminescent dosimeters and Monte-Carlo simulations. Rofo 2008; 180: 1047 – 1053
7 *Stiller W.* Principles of multidetector-row computed tomography. Part 2: Determinants of radiation exposure and current technical developments. Radiologe 2011; 51: 1061 – 1078
8 Radiation-Induced Cataracts, Recommendation by the German Commission on Radiological Protection with Scientific Reasoning, adopted at the 234th meeting of the German Commission on Radiological Protection on 14.05.2009, BAnz no. 180a – 27.11.2009
9 *Kirchhof K, Wohlgemuth WA, Berlis A.* Estimation of the minimum dose required to measure ventricular width in follow-up cranial computed tomography (CCT) in children with hydrocephalus. Fortschr Röntgenstr 2010; 182: 1118 – 1124
10 *Mullins ME, Lev MH, Bove P et al.* Comparison of image quality between conventional and low-dose nonenhanced head CT. AJNR 2004; 25: 533 – 538
11 *Kalender WA.* Computertomografie. Grundlage, Gerätetechnologie, Bildqualität, Anwendungen. 2. Aufl. Publicis Publishing; 2006: 21 – 27, 55 – 63, 102 – 137, 237 – 235
12 *Cohnen M, Fischer H, Hamacher J et al.* CT of the head by use of reduced current and kilovoltage: relationship between image quality and dose reduction. AJNR 2000; 21: 1654 – 1660
13 *Stiller W.* Principles of multidetector-row computed tomography. Part 1: Technical design and physicotechnical principles. Radiologe 2011; 51: 625 – 639
14 *Lira D, Padole A, Kalra MK et al.* Tube potential and CT radiation dose optimization. Am J Roentgenol 2015; 204: W4 – W10

15 *McCollough CH*, *Primak AN*, *Braun N et al.* Strategies for reducing radiation dose in CT. Radiol Clin North Am 2009; 47: 27 – 40
16 *Rybka K*, *Staniszewska AM*, *Biegański T.* Low-dose protocol for head CT in monitoring hydrocephalus in children. Med Sci Monit 2007; 13: 147 – 151
17 *Abdeen N*, *Chakraborty S*, *Nguyen T et al.* Comparison of image quality and lens dose in helical and sequentially acquired head CT. Clin Radiol 2010; 65: 868 – 873
18 *van Straten M*, *Venema HW*, *Majoie CB et al.* Image quality of multisection CT of the brain: thickly collimated sequential scanning versus thinly collimated spiral scanning with image combining. AJNR 2007; 28: 421 – 427
19 *Greess H*, *Wolf H*, *Baum U et al.* Dose reduction in computed tomography by attenuation-based online modulation of tube current: evaluation of six anatomical regions. Eur Radiol 2000; 10: 391 – 394
20 *Huda W*, *Lieberman KA*, *Chang J et al.* Patient size and x-ray technique factors in head computed tomography examinations. II. Image quality. Med Phys 2004; 31: 595 – 601